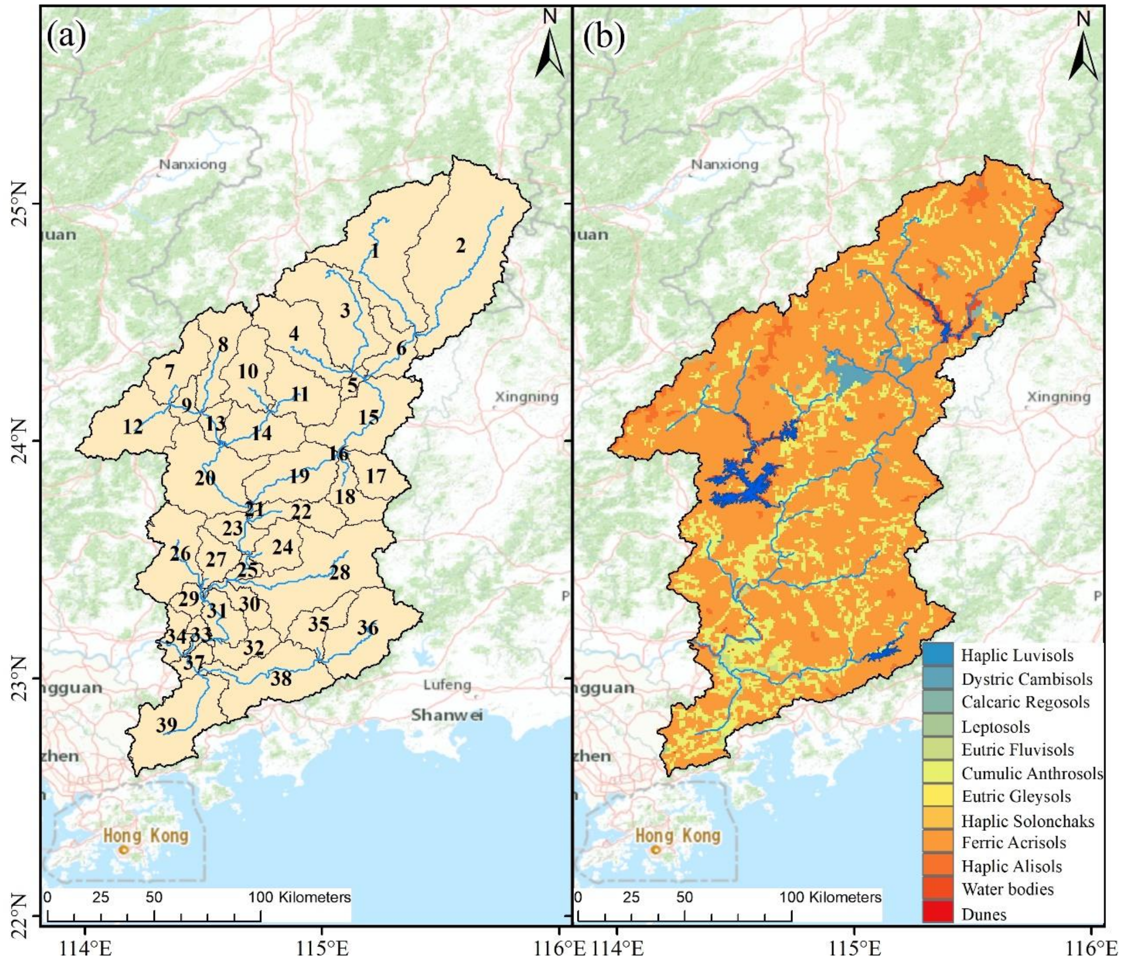

Figure S1. Spatial distribution of sub-basins and soil types in the Dongjiang River basin (Fischer et al., 2008).

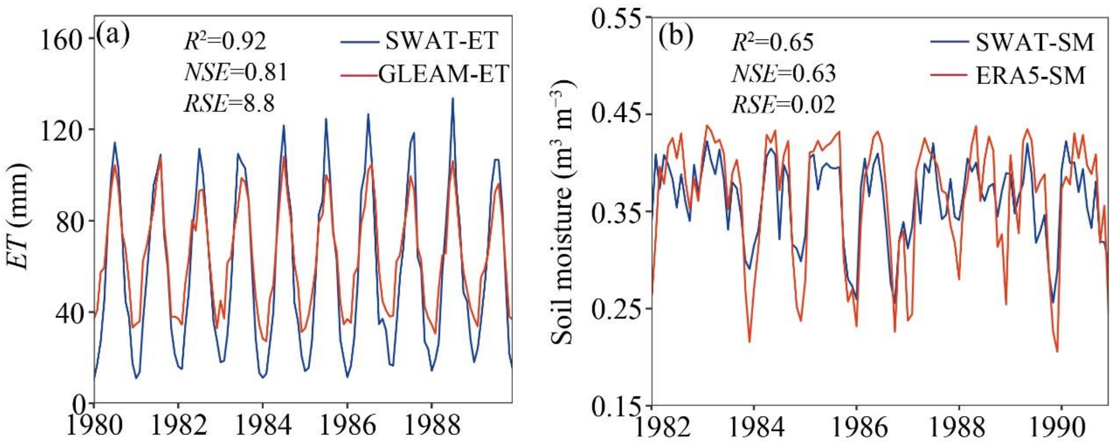

Figure S2. Verification of modeled actual evapotranspiration and soil moisture in the Dongjiang River basin.

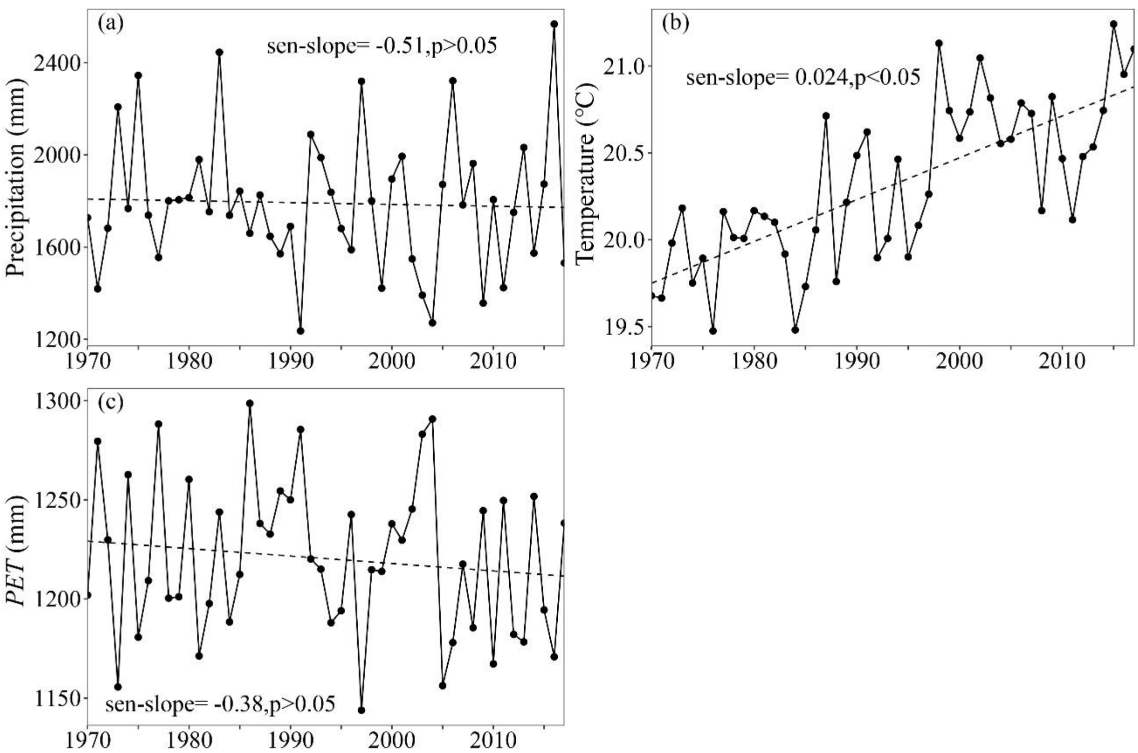

Figure S3. Interannual variation of (a) precipitation, (b) temperature, and (c) potential evapotranspiration in the Dongjiang River basin from 1970 to 2017.

1 Calculation of blue and green water

The HRUs outputs from the SWAT model provide the data to calculate the quantities of *BW* and *GW* in the sub-basin. *BW* is calculated from the summation of water yield (SWAT output *WYLD*) and groundwater storage. The groundwater storage represents the net quantity of water recharge to aquifers (SWAT output *GW_RCHG*) and water discharge from aquifer to the stream (SWAT output *GW_W*) during that time step. *GWF* and *GWS* are equal to the actual evapotranspiration (SWAT output *ET*) and soil moisture (SWAT output *SW*), respectively (Rodrigues et al., 2014). The calculation of the Green Water Index (*GWI*) involves dividing the quantity of *GW* by the combined sum of *BW* and *GW* (Nie et al., 2023; Zang and Liu, 2013).

2 Impacts of climate and LULC changes on blue water for sub-basins

The Figure S4 shows the relative contributions of climate change and land use change to blue water, green water flow, and green water storage variations in sub-basin scale. From 1970 to 2017, when looking at the sub-basins, in 79.0% (50) of the sub-basins, climate change contributed to more than 90.0% of the relative contribution to blue water. In 21.0% (13) of the sub-basins with significant land use changes, the relative contribution of land use change to blue water variation exceeded 10.0%. These were mainly distributed in the middle and lower reaches, such as sub-basins 36 and 39, where land use changes resulted in a decrease in blue water, with relative contributions of 32.8% and 25.5%, respectively. In sub-basin 36, a decrease in cultivated land by 129.6 km^2, an increase in forest land by 115.0 km^2, and an increase in urban land by 14.0 km^2 were observed. In sub-basin 39, a decrease in cultivated land by 118.9 km^2, an increase in forest land by 104.0 km^2, and an increase in urban land by 17.7 km^2 were observed. An increase in built-up area led to a larger impermeable area in the basin, resulting in reduced soil infiltration and increased surface runoff, thereby increasing blue water. An increase in forest land can promote soil infiltration, increase evapotranspiration retention, reduce surface runoff, increase green water flow and green water storage, and decrease blue water. The decrease in blue water in sub-basin 36 indicates that the reduction effect of forest land increase on blue water is stronger than the increase effect of built-up area. Sub-basins 61, 62, and 63 downstream resulted in an increase in blue water with relative contributions of 24.0%, 24.9%, and 11.6%, respectively. The built-up area increased by 16.1 km^2, 59.5 km^2, and 241.0 km^2 in these sub-basins, leading to an increase in basin impermeable area and consequently an increase in blue water in the basin.

In 75.0% (47) of the sub-basins, climate change had a relative contribution of over 90.0% to changes in green water flow. From 1970 to 2017, climate change dominated the impact on green water flow in 61 sub-basins (with relative contributions exceeding 50.0%). In 2 sub-basins, namely, sub-basins 36 and 39, land use change played a dominant role in green water flow changes, with relative contributions of 77.1% and 72.9%, respectively. The likely reason for this is that in sub-basin 36, there was a decrease in cultivated land by 129.6 km^2, an increase in forest land by 115.0 km^2, and an increase in built-up area by 14.0 km^2. In sub-basin 39, cultivated land decreased by 118.9 km^2, forest land increased by 104.0 km^2, and built-up area increased by 17.7 km^2. Vegetation transpiration is the main source of green water flow, and an increase in forest land leads to an increase in vegetation transpiration, thereby increasing basin green water flow. In the northeastern and southwestern parts of the basin, a decrease in forest land led to a decrease in green water flow, with land use contributing over 10.0% to the change. Additionally, in the sub-basin where the Xinfengjiang Reservoir is located, an increase in water body area led to increased water surface evaporation, resulting in an increase in green water flow in the sub-basin. Land use also contributed over 10.0% to the change in green water flow in this sub-basin.

The change in green water storage is relatively smaller compared to blue water and green water flow. In over half of the sub-basins, land use had a relative contribution of over 10.0% to changes in green water storage. In 24.0% (15) of the basins, land use changes had a relative contribution of over 30.0% to changes in green water storage, primarily concentrated in the middle and lower reaches of the basin. There were 4 sub-basins where land use changes contributed over 90.0% to changes in green water storage. From 1970 to 2017, in sub-basins like 36 and 39 in the middle of the basin, cultivated land was converted into forest land, resulting in an increase in green water storage. Land use had a relative contribution of over 90%, which was much larger than the impact of climate change. In the southwestern part of the basin, sub-basins 61, 62, and 63 saw an increase in built-up area, leading to a decrease in green water storage. Their relative contributions to changes in green water storage reached 46.7%, 79.8%, and 48.4%, respectively.

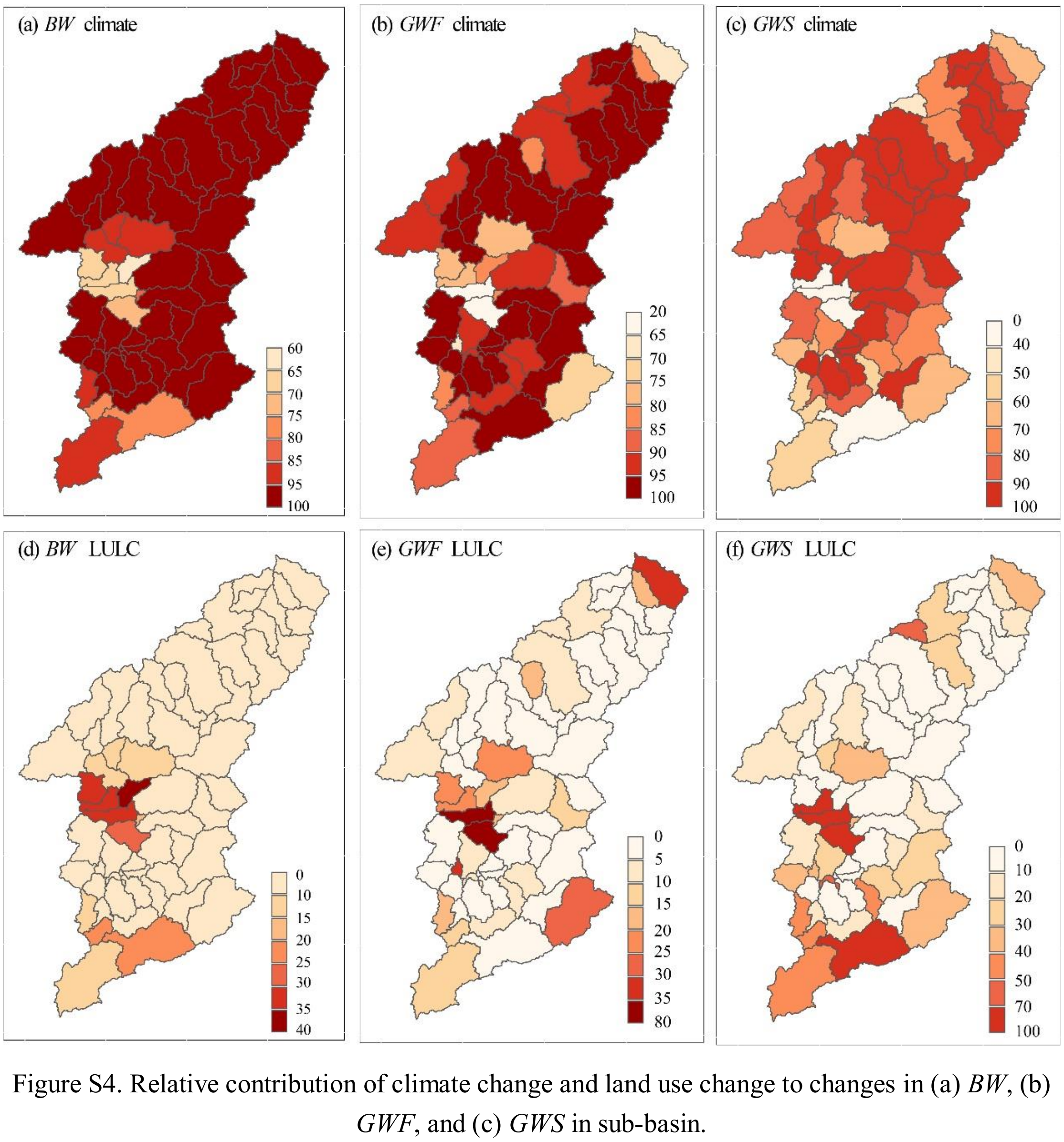

Figure S4. Relative contribution of climate change and land use change to changes in (a) *BW*, (b) *GWF*, and (c) *GWS* in sub-basin.

3 Data availability

The daily meteorological data was obtained from https://data.cma.cn/. The ERA5-land monthly soil moisture data was obtained from https://cds.climate.copernicus.eu/cdsapp#!/dataset/reanalysis-era5-land-monthly-means?tab=overview. The GLEAM monthly actual evapotranspiration data was downloaded from https://www.gleam.eu/. The DEM, population density data, GDP data and land use data were obtained from https://www.resdc.cn/DOI/DOI.aspx?DOIID=33. Soil data was obtained from https://www.fao.org/soils-portal/soil-survey/soil-maps-and-databases/harmonized-world-soil-database-v12/en/.

4 References

Fischer, G., Nachtergaele, F., Prieler, S., Van Velthuizen, H.T., Verelst, L., Wiberg, D., 2008. Global agro-ecological zones assessment for agriculture (GAEZ 2008). IIASA, Laxenburg, Austria and FAO, Rome, Italy 10.

Nie, N., Li, T., Miao, Y., Zhang, W., Gao, H., He, H., Zhao, D., Liu, M., 2023. Asymmetry of blue and green water changes in the Yangtze river basin, China, examined by multi-water-variable calibrated SWAT model. Journal of Hydrology 625, 130099. https://doi.org/10.1016/j.jhydrol.2023.130099

Rodrigues, D.B.B., Gupta, H.V., Mendiondo, E.M., 2014. A blue/green water-based accounting framework for assessment of water security. Water Resources Research 50, 7187–7205. https://doi.org/10.1002/2013WR014274

Zang, C., Liu, J., 2013. Trend analysis for the flows of green and blue water in the Heihe River basin, northwestern China. Journal of Hydrology 502, 27–36. https://doi.org/10.1016/j.jhydrol.2013.08.022